International Journal of Emerging Technology and Advanced Engineering
Volume 3, Special Issue 3: ICERTSD 2013, Feb 2013, pages 146-152
An ISO 9001:2008 certified Int. Journal, ISSN 2250-2459, available online at www.ijetae.com

NUMERICAL STUDY OF GRAVITY EFFECT ON THE NITRIC OXIDE FORMATION IN CO-FLOW METHANE -AIR DIFFUSION FLAME

Arup Jyoti Bhowal[1,*] and Bijan Kumar Mandal[2]

[1]*Department of Mechanical Engineering, Heritage Institute of Technology, Chowbaga Road, Anandapur, P.O. East Kolkata Township, Kolkata- 700 107*

[2]*Department of Mechanical Engineering, Bengal Engineering and Science University, Shibpur, P.O. Botanic Garden, Howrah 711 103, India*

[*]Corresponding author email: arupjyoti.bhowal@heritageit.edu

ABSTRACT
One of the major objectives of current research and development efforts in combustion is to predict and minimize nitric oxide (NO) formation in practical combustion devices. During combustion of fuels having no nitrogen, nitric oxide is formed by three chemical mechanisms. They are Zeldovich or thermal mechanism, Fenimore or prompt mechanism and N_2O-intermediate mechanism. In this work, an attempt has been made to estimate thermal NO formation in methane-air diffusion flame under different reduced gravity levels. The flame has been modeled using the conservation equations of mass, momentum and energy for obtaining temperature and other species concentrations. The NO formation process is decoupled from the hydrocarbon combustion and solved as a post combustion reaction process. It is observed that NO formation increases with the reduction of gravity level below normal gravity level due to temperature rise and velocity reduction in the computational zone. In 0.1 G gravity level, NO concentration values increase to almost three times, compared to the values at normal gravity, at all axial planes.

Keywords: Diffusion flame, gravity, conservation equations, numerical, temperature, velocity, NO formation

1. INTRODUCTION
The major source of useable energy in today's world is met by burning fossil fuels. It is likely that the scenario is not going to change much, even though, a lot of progress has been made and continuous work is going on in harnessing non conventional sources of energy e.g. solar power, nuclear energy, ocean energy etc. However, one serious limitation with the energy obtained from fossil fuels is that they generate air pollutants such as soot and different toxic and greenhouse gases like NO_x, SO_x and CO_2 , which have harmful effects on human being as well as on earth's climate. The oxides of nitrogen are one of the most harmful pollutants. The principal oxides of nitrogen found in atmosphere are nitric oxide (NO), nitrogen dioxide (NO_2) and nitrous oxide (N_2O). NO and NO_2 are collectively called NOx, which contributes to photochemical smog, acid rain, degradation of visibility and fine particulate. On the other hand, N_2O has direct effect on the stratospheric ozone layer depletion and global warming. Significant amount of NO_x comes from the combustion of fossil fuels. Nitrogen oxide (NO) and other nitrogen oxides (NO_x) react with other chemicals in the air to form nitrogen dioxide. Nitric acid and nitrous acid are formed with presence of moisture in air and in the lungs of human beings. This is highly corrosive to the pulmonary system in the body. The main health hazard of nitrogen dioxide is, therefore, on the respiratory system. Inhalation of nitrogen dioxide by children increases their risk of respiratory infection and may lead to poorer lung function in later life. There is also an association between nitrogen dioxide concentrations in the air and increases in daily mortality and hospital admissions for respiratory diseases. Nitrogen dioxide is toxic to plants in short-term concentrations of 120 $\mu g/m^3$. It reduces plant growth. When sulphur dioxide and ozone are also present, the effects on vegetation are worse. Nitrogen dioxide can form secondary particles called nitrates that cause haze and reduce visibility.

Over the last 50 years, with the advancement of industrialization, NO_x emission regulating acts have become more and more stringent resulting in the development of advanced NO_x control technology accompanied by new diagnostic techniques. Out of all the oxides of nitrogen, NO is the most significant one formed during hydrocarbon combustion. During combustion of fuels having no nitrogen, NO is formed by three chemical mechanisms. They are Zeldovich or thermal mechanism [1], Fenimore or prompt mechanism [2] and N_2O-intermediate mechanism.

Presented at International Conference on Energy Resources and Technologies for Sustainable Development, 07-09 February 2013, Howrah, India.

ISSN 2250-2459, *Volume 3, Special Issue 3: ICERTSD 2013, Feb 2013, pages 146-152*

The thermal mechanism dominates in high temperature combustion whereas Fenimore mechanism is particularly significant in rich combustion. The third one, the N_2O- intermediate mechanism plays an important role in NO formation in very lean, low-temperature combustion process. Peters and Donnerhack [3] studied the NO_x production in a turbulent diffusion flame and observed the dependence of the NO_x emissions on Reynolds number and Froude number. Chen and Driscoll [4] studied the effects of coaxial air velocity, Reynolds number and Damkohler number on the total nitric oxide emissions of hydrogen and methane diffusion flames.

Phuoc *et al.* [5] reported from their experimental investigation of a steady methane-air jet flame surrounded by a shroud of combustion air that NO_x emissions decreased substantially with the increase of air velocity and lowering of fuel velocity. To study the effects of air-side and fuel-side diluent addition on nitric oxide emissions, Feese and Turns [6] numerically simulated a counterflow laminar methane-air diffusion flame using full kinetics and made calculations of NOx emission indices for various conditions. N_2 diluent was added either on the fuel or air-side of the flame for conditions of either fixed initial velocity or fixed fuel mass flux. They observed that NO emissions decreased for air-side as well as fuel-side dilution. Their experimental results with laminar flames showed that the fuel-side diluent gave greater NO_x emissions than air-side diluent addition.

Beltrame *et al.* [7] investigated NO and soot formation both numerically and experimentally in oxygen-enriched methane counterflow diffusion flames. The thermal mechanism of NO production was found to be the major contributor near the maximum temperature region. The prompt mechanism contributed significantly to NO formation in the fuel rich regions. The prompt mechanism also contributed to NO destruction. Effect of pressure on NO emission in high temperature and diluted air conditions was numerically studied by Sohn *et al.* [8]. They found that the dilution lowered the flame temperature appreciably resulting in low production rate of NO. A numerical and experimental investigation of the effects of air preheat were studied by Fuse *et al.* [9]. They observed that the increase in air temperature increased the NO formation in diffusion flames. They further found that NO formation can be decreased, even with high air temperature, if the oxidizer is vitiated with inert gas to reduce the oxygen concentration in it. Costa *et al.* [10] investigated unconfined, vertical, turbulent methane jet diffusion flames issuing from a straight tube into quiescent air at atmospheric pressure and temperature, and focused on NO_x emissions. They found that the transition from buoyancy to momentum controlled turbulent jet diffusion flames occurs at a Froude number of about 10^4. The effects of highly preheated air on NO formation on a methane-air two dimensional laminar diffusion jet flame was numerically studied with detailed chemistry by Ju and Niioka [11].

Their computed results showed that NO formation by both thermal and prompt mechanisms increased significantly with the increase of air temperature. It is noted that not much of work is available in the literature on the formation of nitric oxide under reduced gravity conditions. This motivated the authors to investigate numerically the effects of lower gravity on NO formation in a methane-air co-flow diffusion flame.

2. MATHEMATICAL MODEL

The physical model of the combustion system is as shown in figure 1. The burner is composed of two concentric vertical tubes. The fuel is admitted as a central jet through the inner tube and air as a co-flowing annular jet through the outer tube. The inner fuel tube diameter is 12.7 mm and the outer tube diameter is 50.4 mm. The inner tube wall is considered to be thin and its thickness is neglected for the computation. The dimensions are the same as those of the earlier experimental work of Mitchell *et al.* [12] and the numerical work of Smooke *et al.* [13]. The two streams diffuse into each other at the outlet of the inner tube in order to produce a flammable mixture of fuel and air. A cylindrical shield of diameter 50.4 mm defines an impervious outer boundary (wall) of the axisymmetric system. The fuel is considered here to be methane gas (CH_4). Numerical simulations have been performed and presented on one side of the axis only with the consideration of the axisymmetric geometry.

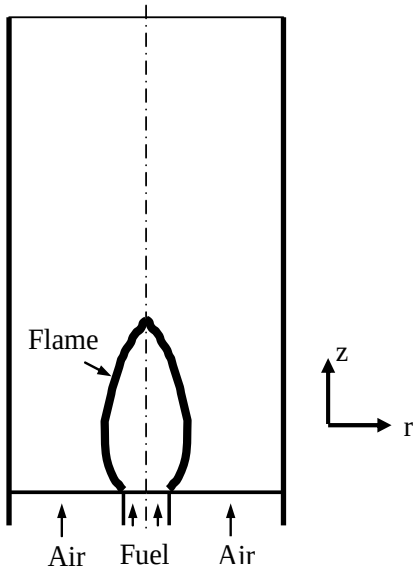

Fig. 1. Physical model of the flame

The combustion process is simulated with a detailed numerical model and finding solutions of the governing equations for reacting flow with appropriate boundary conditions. The governing equations considered here are based on the conservation of overall mass, species concentration, axial momentum, radial momentum and energy. The equations have been written in cylindrical co-ordinate system.

ISSN 2250-2459, *Volume 3, Special Issue 3: ICERTSD 2013, Feb 2013, pages 146-152*

Since the flow is symmetric, computation in the axial and the radial directions only have been performed making the analysis appear a two dimensional one. The conservation equations with transient terms for mass, radial momentum, axial momentum, species concentrations and energy are presented in Eq.(1) to Eq.(5) respectively.

$$\frac{\partial \rho}{\partial t}+\frac{1}{r}\frac{\partial}{\partial r}(r\rho v_r)+\frac{\partial}{\partial z}(\rho v_z)=0 \tag{1}$$

$$\frac{\partial}{\partial t}(\rho v_r)+\frac{1}{r}\frac{\partial}{\partial r}\left(r\rho v_r^2\right)+\frac{\partial}{\partial z}(\rho v_r v_z)=-\frac{\partial p}{\partial r}+\frac{2}{r}\frac{\partial}{\partial r}\left(r\mu\frac{\partial v_r}{\partial r}\right)-\frac{2}{r}\mu\frac{v_r}{r^2}+\frac{\partial}{\partial z}\left\{\mu\left(\frac{\partial v_z}{\partial r}+\frac{\partial v_r}{\partial z}\right)\right\}-\frac{2}{3}\frac{\partial}{\partial r}\left(\mu\left(\frac{\partial v_r}{\partial r}+\frac{v_r}{r}+\frac{\partial v_z}{\partial z}\right)\right) \tag{2}$$

$$\frac{\partial}{\partial t}(\rho v_z)+\frac{1}{r}\frac{\partial}{\partial r}(r\rho v_r v_z)+\frac{\partial}{\partial z}\left(\rho v_z^2\right)=-\frac{\partial p}{\partial z}+\frac{1}{r}\frac{\partial}{\partial r}\left\{r\mu\left(\frac{\partial v_z}{\partial r}+\frac{\partial v_r}{\partial z}\right)\right\}+2\frac{\partial}{\partial z}\left(\mu\frac{\partial v_z}{\partial z}\right)-\frac{2}{3}\frac{\partial}{\partial z}\left\{\mu\left(\frac{\partial v_r}{\partial r}+\frac{v_r}{r}+\frac{\partial v_z}{\partial z}\right)\right\}+\rho g \tag{3}$$

$$\frac{\partial}{\partial t}\left(\rho C_j\right)+\frac{1}{r}\frac{\partial}{\partial r}\left(r\rho v_r C_j\right)+\frac{\partial}{\partial z}\left(\rho v_z C_j\right)=\frac{1}{r}\frac{\partial}{\partial r}\left(r\rho D_{jm}\frac{\partial C_j}{\partial r}\right)+\frac{\partial}{\partial z}\left(\rho D_{jm}\frac{\partial C_j}{\partial z}\right)+\dot{S}_{cj} \tag{4}$$

$$\frac{\partial}{\partial t}(\rho h)+\frac{1}{r}\frac{\partial}{\partial r}(r\rho v_r h)+\frac{\partial}{\partial z}(\rho v_z h)=\frac{1}{r}\frac{\partial}{\partial r}\left(r\frac{\lambda}{c_p}\frac{\partial h}{\partial r}\right)+\frac{\partial}{\partial z}\left(\frac{\lambda}{c_p}\frac{\partial h}{\partial z}\right)+\frac{1}{r}\frac{\partial}{\partial r}\left[r\frac{\lambda}{c_p}\sum_{j=1}^{n}h_j\left(Le_j^{-1}-1\right)\frac{\partial C_j}{\partial r}\right]+\left[\frac{\lambda}{c_p}\sum_{j=1}^{n}h_j\left(Le_j^{-1}-1\right)\frac{\partial C_j}{\partial z}\right] \tag{5}$$

where, C_j is the mass fraction of the respective species and D_{jm} is the diffusion coefficient of the species in a binary mixture of that species and nitrogen and Lej is the local Lewis number defined as

$$Le_j=\frac{\lambda}{c_p}\frac{1}{\rho D_{jm}} \tag{6}$$

The source term, $\dot{S}_{cj}$ is the rate of production or destruction of the species j per unit volume due to chemical reaction. The temperature dependence of viscosity (μ), thermal conductivity (λ), mass diffusivity (D_{jm}) and specific heat (c_p) has been taken into account using suitable correlations available in the literature. The axial and radial directions are denoted by z and r respectively. The conservation equation for chemical species is solved for five gaseous species, viz. CH_4, O_2, CO_2, CO and H_2O. The concentration for N_2 is obtained by difference.

The variations of the thermodynamic as well as transport properties of component gases and the mixture with temperature have been taken care of by the use of suitable correlations. The details of these can be obtained from the work of Mandal *et al.* [14].

2.1 Thermal NO Model

As NO is the main oxide of nitrogen and constitutes the major share of NO_x formed in a combustion process, its formation through the thermal route is calculated following Zeldovich mechanism in a manner similar to that adopted by Ramos [15]. Since the initial step of Zeldovich reaction mechanism involves a very high activation energy, it requires a very high temperature to initiate the reaction. Moreover the reaction kinetic is slower than the kinetics of the chemical reaction of fuel and therefore, the NO formation process can be decoupled from the hydrocarbon combustion and can be solved as post combustion reaction process. The NO formation is governed by the following equations.

$$O_2+M\Leftrightarrow O+O+M \tag{7}$$

$$O+N_2\Leftrightarrow NO+N \tag{8}$$

$$N+O_2\Leftrightarrow NO+O \tag{9}$$

A steady-state assumption, made for the calculation of N- atoms, gives

$$\frac{dy_N}{dt}=0 \tag{10}$$

The O-atom is assumed to be in equilibrium with the O_2 molecule as

$$M+O_2\Leftrightarrow M+2O \tag{11}$$

where M is a third body.

The rate of formation of NO is calculated as

$$\frac{dy_{NO}}{dt}=K_1y_{N_2}y_O-K_2y_{NO}y_N+K_3y_Ny_{O_2}-K_4y_{NO}y_O \tag{12}$$

where the values of y_N and y_O are obtained from the assumptions given in equations (10) and (11). The specific reaction rates K_1, K_2, K_3 and K_4 for the above reactions have been taken from the work of Ramos [15]. The specific conservation equation for NO is solved with its rate of formation as the source term for finding NO concentration within the combustor as well as at the combustor exit.

ISSN 2250-2459, *Volume 3, Special Issue 3: ICERTSD 2013, Feb 2013, pages 146-152*

3. NUMERICAL SOLUTION

The conservation equations for the reacting flow are solved using a numerical algorithm called SOLA. The algorithm is based on primitive variables and the variables are defined following a staggered grid arrangement. A non-uniform size grid system is generated. After grid independence test, a numerical mesh with 85×41 grid nodes is selected. The diffusion terms are discretized by a central differencing scheme, whereas the advection terms are discretized by a hybrid differencing schemes.

3.1 Boundary Conditions

Boundary conditions at the inlet are given separately for the fuel stream at the central jet and the air stream at the annular co-flow. The temperatures of inlet fuel and that of the air are taken as 300 K. In conformation with the conditions used by Mitchell *et al.* [12] and Smooke *et al.* [13], the fuel flow rate is taken as 3.71×10^{-6} kg/s and the air flow rate is taken as 2.214×10^{-4} kg/s. Fully developed boundary conditions for the variables are considered at the outlet. In case of reverse flow at the outlet plane, which occurs in the case of buoyant flame, the stream coming in from the outside is considered to be ambient air. Axisymmetric condition is considered at the central axis, while at the wall a no-slip, adiabatic and impermeable boundary condition is adopted. At the inlet to the computational zone, NO concentration is taken as zero.

4. RESULTS AND DISCUSSIONS

The pollutant formation under study in the present investigation is the thermal NO. Thermal NO is formed in the high temperature zone, where both N_2 and O_2 exist. The laminar confined axisymetric methane-air diffusion flame with non-preheated air was simulated and numerical results were obtained for three gravity levels namely; 1.0 G (normal gravity), and reduced gravities of 0.50 G and 0.10 G. The flame shape and the distributions of temperature and NO concentrations have been presented for these three gravity levels

4.1. Flame Height

Figure 2(a) to figure 2(c) show the shape of flame front for three gravity levels namely, of 1.0 G, 0.50 G, and 0.10 G. The flame front is described by the volumetric heat release rate contour having value 1% of the maximum local volumetric heat release rate due to chemical reaction. It may be seen from the figure 2(a) that the flame height is around 12 cm for gravity level of 1.0 G.. It is further observed that the flame height reduces progressively as one goes for lower gravity levels with the flame height becoming around 10 cm for gravity level of 0.10 G, as seen in these figures. The flame also flattens out in radial direction for lower gravity levels. This is very prominently observed in the bulge of the flame for 0.10 G. This is because of the lower buoyancy force and also lower recirculation of ambient air at lower gravity levels. This gives rise to a near spherical flame shape as gravity level deceases.

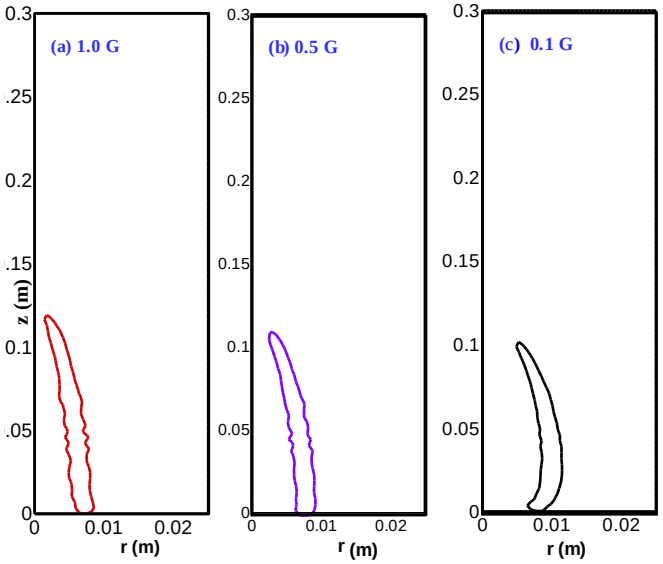

Fig. 2 Shape of the flame fronts for three different gravity levels: (a) 1.0 G, (b) 0.50 G and (c) 0.10 G

4.2 Temperature Distributions

Figure 3(a) to figure 3(c) show the radial distributions of temperature for three gravity levels namely, of 1.0 G, 0.50 G, and 0.10 G, each graph showing temperature distribution at four axial heights of 5 cm, 10 cm, 12 cm and 20 cm respectively above the burner tip. In other words, each figure shows the radial distribution of temperature for a particular gravity level at four different heights.

It is found from the plots that at all gravity levels, as mentioned above, the maximum temperature encountered is around 2250 K. Also the radial position of the peak temperature for the individual heights of 5 cm and 10 cm on any particular plot is positioned away from the axis. This position further moves away from the axis as one goes for lower gravity levels. For the individual heights of 12 cm and 20 cm on any particular plot, the peak temperature position is always located on the axis. It is also observed that on the axis, the highest temperature occurs at around 12 cm height for gravity levels of 1.0 G and 0.50 G and this means that the flame height for these two gravity levels is 12 cm. For the lower gravity level of 0.10 G the flame height may be seen to be around 10 cm as the peak centreline temperature is observed near 10 cm axial height above the burner tip

4.3 NO Distribution for Different Gravity Levels

Figure 4(a) to figure 4(c) show the radial distributions of NO concentration for three gravity levels namely, of 1.0 G, 0.50 G, and 0.10 G, each graph showing concentration distribution at four axial heights of 5 cm, 10 cm, 15 cm and 20 cm respectively above the burner tip. In all these plots, it is observed that the value of peak NO concentration increases from 5cm to 10 cm height and then it decreases with increase of height. It is further seen that in general values of concentration

ISSN 2250-2459, *Volume 3, Special Issue 3: ICERTSD 2013, Feb 2013, pages 146-152*

increase as one goes for lower gravity level. For gravity levels of 1.0 G and 0.5 G, the curves become flatter after a radial distance of approx. 15 mm. in line with temperature distribution (which also show a similar i.e. flat distribution for these two gravity levels) as seen in fig. 3. In 0.1G gravity level, the concentration values increase almost 3 times for all heights, compared to the values at normal gravity level of 1.0 G.

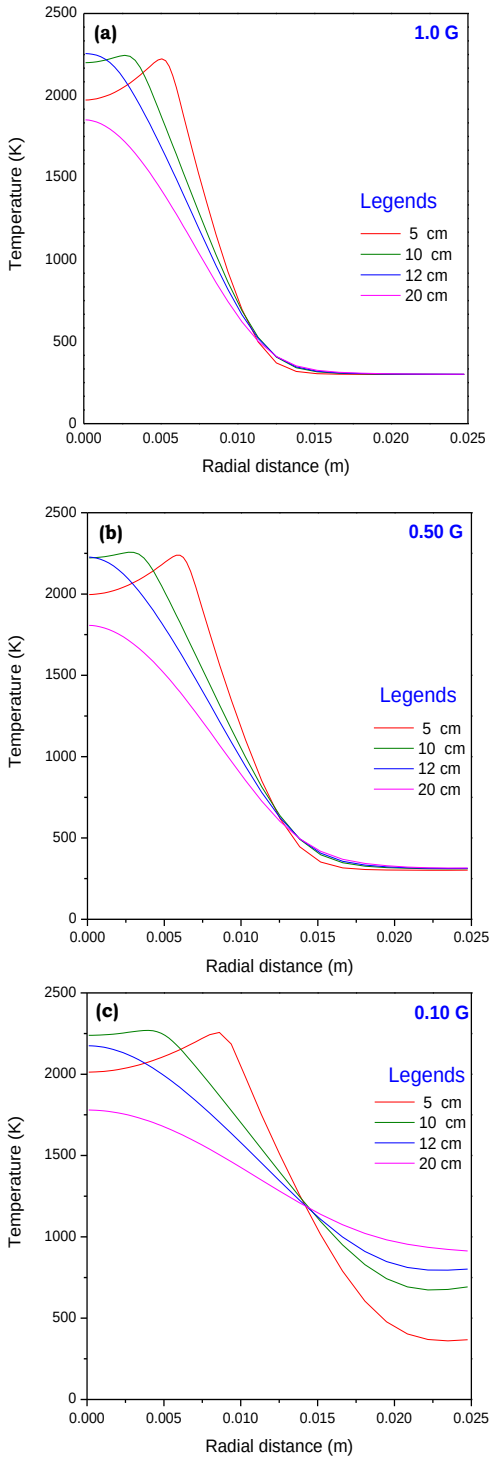

Fig. 3. Radial distributions of temperature at different axial planes, for three gravity levels: (a) 1.0 G (b) 0.50 G and (c) 0.10 G

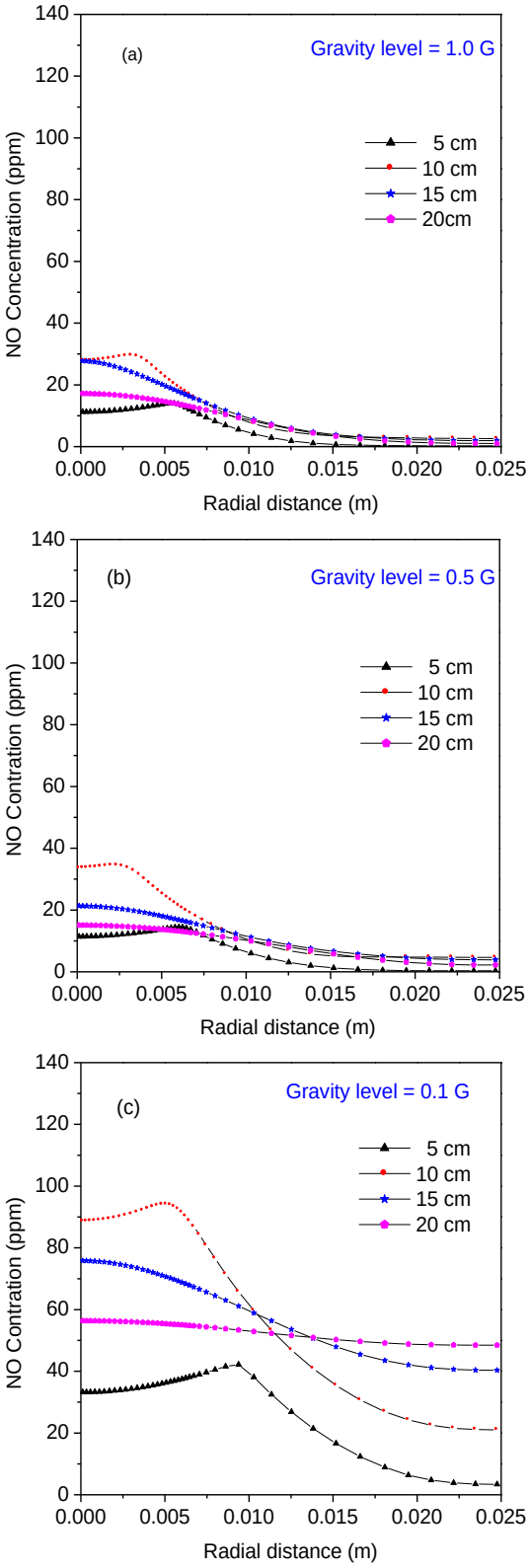

Fig. 4. Radial distributions of NO concentration at different axial planes, for gravity levels: (a) 1.0 G, (b) 0.50 G and (c) 0.10 G

4.4 Comparison of NO at Different Axial Planes

Figure 5(a) to figure 5(d) show the radial distributions of NO concentration for four axial heights, namely, 5 cm, 10 cm, 15 cm and 20 cm respectively above the

ISSN 2250-2459, *Volume 3, Special Issue 3: ICERTSD 2013, Feb 2013, pages 146-152*

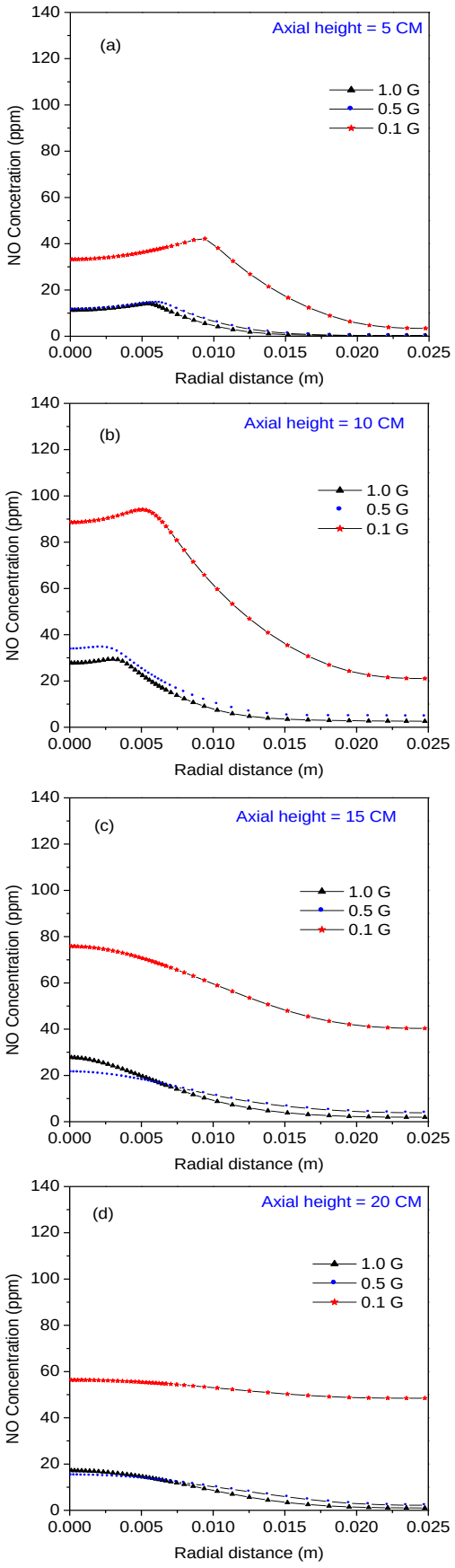

Fig. 5 Radial distributions of NO concentration at different axial heights: (a) 5 cm (b) 10 cm (c) 15 cm and (d) 20cm

burner tip for three gravity levels of 1.0 G, 0.50 G and 0.10 G. Each figure shows the radial distribution of NO concentration at a particular height for all the three gravity levels, as already mentioned.

It is seen that for all heights, the values are higher for lower gravity levels. It is also seen that the values for all gravity levels increase from 5 cm height to 10 cm height then go down for higher heights of 15 cm and 20 cm. Values are markedly higher – about three times – for gravity level of 0.10 G. This can be explained from the temperature distribution. The rate of formation of NO is very much temperature dependent and it increase with the rise in temperature. As the temperature goes up at lower gravity level, the effect on enhanced rate of NO formation is clearly observed in all the plots at the gravity level of 0.10 G. At lower gravity and higher heights, distribution shows a flatter tendency because the mixture of gases has a more uniform distribution in absence of recirculation of ambient air from the exit plane resulting in diffusion of NO towards the wall.

5. CONCLUSIONS

A numerical experimentation has been performed on a laminar confined axisymetric methane-air diffusion flame under reduced gravity levels and results compared with those under normal gravity. The results have been presented in terms of flame height, temperature distribution and NO concentration. The flame height is found to be around 12 cm for normal gravity and it reduces with the decrease of gravity levels. The flame height becomes approximately 10 cm for gravity level of 0.10 G. High temperature zone is limited to a small radial distance in case of comparatively higher gravity levels. However, at the gravity levels of 0.10 G, relatively high temperature prevails in the region near the outer boundary wall also. It is also seen that in general values of concentration increase as one goes for lower gravity level. In 0.1 G gravity level, the NO concentration values increase almost 3 times for all heights. It is also observed that the distribution of NO concentration becomes almost flat at higher heights and lower gravity because there is no recirculation of ambient air from the exit plane.

REFERENCES

1. Zeldovich, Y.B., 1946, "The Oxidation of Nitrogen in Combustion Explosions", Acta Physiochimica, U.S.S.R. 21: 577 - 628.
2. Fenimore, C.P. and Jones, G.W., 1957, "Nitrio Oxide Decomposition at 2200 – 2400 K", Journal of Physical Chemistry, 61: 654 – 657
3. Peters, N. and Donnerhack, S., 1981, "Structure and Similarity of Nitric Oxide Production in Turbulent Diffusion Flames", *Eighteenth Symposium (International) on Combustion, The Combustion Institute, Pittsburgh*, p 33.
4. Chen, R.H. and Driscoll, J.F., 1990, "Nitric Oxide Levels of Jet Diffusion Flames : Effects of Coaxial Air and Other Mixing Parameters", *Twenty-Third*

ISSN 2250-2459, *Volume 3, Special Issue 3: ICERTSD 2013, Feb 2013, pages 146-152*

Symposium (International) on Combustion, The Combustion Institute, Pittsburgh, p 281

5. Phuoc, T.X., Mathur, M.P., Ekmann, J.M. and White, F.P., 1997, "NO_x Emissions of a Jet Diffusion Flame which is Surrounded by a Shroud of Combustion Air", Optical Diagnostics in Engineering, 2: 32 - 43.
6. Feese, J.J. and Turns, S.R., 1998, "Nitric Oxide Emissions from Laminar Diffusion Flames: Effects of Air-side versus Fuel-side Diluent Addition", Combustion and Flame, 113: 66 - 78.
7. Beltrame, P. P., Merchan, W.M., Saveliev, A., Fridman, A., Kennedy, L.A., Petrova, O., Zhdanok, S., Amouri, F. and Charon, O., 2000, "Soot and NO Formation in Methane-Oxygen Enriched Diffusion Flames", Combustion and Flame, 124: 295 - 310.
8. Sohn, C.H., Jeong, I.M. and Chung, S.H., 2002, "Numerical Study of the Effects of Pressure and Air-Dilution on NO Formation in Laminar Diffusion Flames of Methane in High Temperature Air", Combustion and Flame, 130: 83 - 93.
9. Fuse, R., Kobayashi, H., Ju, Y., Maruta, K. and Niioka, T., 2002, "NO_x Emission from High Temperature Air/Methane Counterflow Diffusion Flame", International Journal of Thermal Sciences, 41: 693-698.
10. Costa, M. , Parente, C. and Santos, A., 2004, "Nitrogen oxides emissions from buoyancy and momentum controlled turbulent methane jet diffusion flames", Experimental Thermal and Fluid Science, 28 : 729–734.
11. Ju, Y. and Niioka, T., 1997, "Computation of NO_x Emission of a Methane-Air Diffusion Flame in a Two-Dimensional Laminar Jet with Detailed Chemistry", Combustion Theory and Modelling, 1: 243 - 258.
12. Mitchell, R.E., Sarofim, A.F. and Clomburg, L.A. 1980, "Experimental and Numerical Investigation of Confined Laminar Diffusion Flames", Combustion and Flame, 37: 227 - 244.
13. Smooke, M.D., Mitchell, R.E. and Keys, D.E., 1989, "Numerical Solution of Two-Dimensional Axisymmetric Laminar Diffusion Flames", Combustion Science and Technology, 67: 85 - 122.
14. Mandal, B. K., Sarkar, A. and Datta, A., 2008, "Transient Development of Flame and Soot Distribution in Laminar Diffusion Flame With Preheated Air", Journal of Engineering for Gas Turbines and Power, 131: 031501-1 031501-9
15. Ramos, J. J., 1985, "A Numerical Study of a Swirl Stabilized Combustor", Journal of Non-Equilibrium Thermodynamics, 10: 263 - 268

AUTHOR BIOGRAPHY

Mr Arup Jyoti Bhowal did his B Tech (Hons) in Mechanical Engineering from IIT Kharagpur and joined industries thereafter. He later came to teaching profession and completed masters degree in Mechanical Engineering and registered for Ph D work from Bengal Engineering and Science University, Shibpur, India. He is currently an Assistant Professor in Mechanical Engineering at Heritage Institute of Technology, Kolkata. His research interest is combustion and alternative fuels. He has published several research papers in international conferences and journals.

Dr. Bijan Kumar Mandal is a Professor in Mechanical Engineering at Bengal Engineering and Science University, Shibpur, India. He received his B.Tech. (Hons.) and M.Tech. in Mechanical Engineering from the Indian Institute of Technology, Kharagpur, India. He completed his PhD in Engineering from Jadavpur University, India. His research areas of interest are IC engine fuels, combustion and combined cycles. He has published many research papers in the field of combustion, energy and heat transfer.

.